Journal of Catalysis 364 (2018) 166–173

Contents lists available at ScienceDirect

Journal of Catalysis

journal homepage: www.elsevier.com/locate/jcat

Water activation by single Pt atoms supported on a Cu_2O thin film

Andrew J. Therrien [a], Kyle Groden [b], Alyssa J.R. Hensley [b], Alex C. Schilling [a], Ryan T. Hannagan [a], Matthew D. Marcinkowski [a], Alex Pronschinske [a], Felicia R. Lucci [a], E. Charles H. Sykes [a,*], Jean-Sabin McEwen [b,c,d,e,f,*]

[a] Department of Chemistry, Tufts University, Medford, MA 02155, United States
[b] The Gene and Linda Voiland School of Chemical Engineering and Bioengineering, Washington State University, Pullman, WA 99164, United States
[c] Department of Physics and Astronomy, Washington State University, Pullman, WA 99164, United States
[d] Department of Chemistry, Washington State University, Pullman, WA 99164, United States
[e] Department of Biological Systems Engineering, Washington State University, Pullman, WA 99164, United States
[f] Institute for Integrated Catalysis, Pacific Northwest National Laboratory, Richland, WA 99352, United States

ARTICLE INFO

Article history:
Received 15 January 2018
Revised 2 April 2018
Accepted 21 April 2018

Keywords:
Single atom catalysis
Platinum
Water activation
Water scrambling
Oxidized copper
Density functional theory
Temperature programed desorption

ABSTRACT

Recent advances in single atom catalysis have sparked interest in their use as low-cost and high-efficiency catalysts in a wide variety of reactions. One such reaction that has been heavily studied with single atom catalysts is the water gas shift reaction. In addition, water participates in a rich variety of other industrially important catalytic processes, such as steam reforming reactions. However, much debate surrounds the structure and activity of single atoms toward water gas shift chemistry. By taking a model study approach, we determine the influence of atomically dispersed Pt atoms on the activation of water. Using a thin film Cu_2O/Cu(1 1 1) support, water activation is probed via isotopic scrambling temperature programed desorption experiments. We determine that the presence of supported single Pt atoms on the thin Cu_2O film will facilitate the low-temperature activation of water. Theory offers a viable water scrambling pathway on the supported Pt atoms, detailing the dynamic relationship between water, the Pt atom, and the support. The results reveal that single Pt atoms are capable of O-H bond activation when water interacts with such a catalyst.

1. Introduction

Supported single atoms are a rapidly growing class of catalysts that have shown promise as highly active, selective, and inexpensive materials [1–3]. The water gas shift reaction catalyzed by supported single atoms has been particularly heavily studied [4–10]. Interestingly, the reaction has been found to display remarkably similar reactivity on a variety of active single atom and support combinations [4–8]. Pt is one of the catalytic elements found to be active for the water gas shift reaction [6,9]. The reactivity of Pt single atoms [6,9,10], Pt clusters [11–16], and Pt alloys [17,18] toward water gas shift catalysis have previously been studied. However, in those cases, the optimal structure of Pt for the water gas shift reaction has been widely debated, with arguments made both for and against Pt single atoms versus Pt nanoparticles [6,9,15,19,20]. Here, we take a model study approach, creating isolated Pt single atoms dispersed on a well-defined support, to address fundamental questions of structure and reactivity. We have previously used this approach to demonstrate the oxidation of CO by Pt single atoms [21], and now use a similar methodology to study the activation of water.

The model support used in this study is a thin film Cu_2O(1 1 1)-like layer known as the "29" oxide. The "29" oxide is reproducibly formed by controlled oxidation of Cu(1 1 1), forming a single layer oxide film on the surface [22–25]. The atomic structure of the "29" oxide has been previously investigated through a combination of scanning tunneling microscopy (STM) and density functional theory (DFT) [24,25], and guided by previous surface science work [26]. The proposed structure of the "29" oxide is made up of six hexagonal rings, consisting of linear O-Cu-O bonds, per surface unit cell [24]. Within five of these porous rings resides an additional O adatom bound to the Cu(1 1 1) substrate [24]. In order to first understand water adsorption on the "29" oxide support, previous surface science studies can serve as a guide. Water interactions on oxidized Cu also have catalytic implications, as Cu-based

* Corresponding authors at: Department of Chemistry, Tufts University, Medford, MA 02155, United States (E.C.H. Sykes); The Gene and Linda Voiland School of Chemical Engineering and Bioengineering, Washington State University, Pullman, WA 99164, United States (J.-S. McEwen).

E-mail addresses: charles.sykes@tufts.edu (E. Charles H. Sykes), js.mcewen@wsu.edu (J.-S. McEwen).

https://doi.org/10.1016/j.jcat.2018.04.024
0021-9517/

catalysts are used industrially for the low-temperature water gas shift reaction and methanol steam reforming [27–36]. Generally, interfacial water structures are very complex, and have been heavily studied due to their broad application in many technologies [37–39]. Studies on single-crystal metal oxides have found that water molecules generally dissociate at defect sites on oxides, and in certain cases cause the surface to become hydroxylated [37–43]. The "29" oxide surface is largely defect free, with a defect density of approximately 0.02% of a monolayer with respect to the Cu(1 1 1) surface [24], which facilitates non-dissociative water adsorption. Water adsorption on oxidized Cu substrates has been studied by spectroscopic techniques [30,44,45]. Under near-ambient pressures, small amounts of surface hydroxyls were detected upon water adsorption to polycrystalline Cu_2O thin films [30], and water exposure under vacuum conditions also caused hydroxyl formation at submonolayer coverages of O on Cu(1 1 1) [44]. However, continuous and more complete Cu_2O films, such as the "29" oxide, have shown no evidence of water dissociation [44]. Recently, cyclic water hexamers on partially oxidized Cu(1 1 1) studied by STM were found to be surprisingly stable for non-dissociative water adsorption [46]. These results are also in line with DFT calculations that conclude water dissociation to be unfavorable on intact Cu_2O(1 1 1) [47,48]. Further work suggests that defects are the only active sites for water dissociation on bulk Cu_2O(1 1 1) [44,49].

The primary focus of this work is to study the activity of Pt single atoms toward water activation. To understand water adsorption and activation on supported single atoms, we must first investigate water adsorption and desorption on the bare "29" oxide. With this information, the "29" oxide surface will serve as a model support to assess the activity of atomically dispersed Pt atoms. Furthermore, isotopic labeling of the "29" oxide provides a way to quantify the degree of water activation. This approach allows for accurate DFT modeling, and in combination with experiment, this work provides fundamental insight into water interactions on supported Pt single atoms and the role of the support.

2. Methods

2.1. Temperature programed desorption (TPD)

TPD experiments were carried out in an ultra-high vacuum (UHV) chamber with a base pressure of $<1 \times 10^{-10}$ mbar. The chamber was equipped with a quadrupole mass spectrometer (Hiden) and the Cu(1 1 1) crystal was able to be cooled to 85 K with liquid nitrogen and resistively heated to 750 K. The Cu(1 1 1) crystal was cleaned by Ar^+ sputtering and annealing to 750 K. The "29" oxide film was formed by exposure to O_2 gas (Airgas, USP grade), or $^{18}O_2$ (Aldrich, 97%) for isotopic scrambling experiments, at a pressure of 5×10^{-6} mbar for 3 min at a sample temperature 650 ± 20 K. The formation of the "29" oxide was verified by low energy electron diffraction (OCI Vacuum Microengineering). Pt depositions were performed on a cooled "29" oxide sample held at 85 K, using a Focus GmbH EFM3 electron beam evaporator. One monolayer (ML) is defined as the packing density of Cu(1 1 1), 1.77×10^{15} atoms cm^{-2}. High precision leak valves allowed for accurate exposure of deionized water obtained from a Nanopure water system, which was further purified by first boiling the water (to reduce the amount of dissolved gas in the liquid) and then proceeding with freeze-pump-thaw cycles. The background pressure of water in the UHV chamber was also used as a deposition source of water for low coverage experiments. TPD experiments were performed with a linear heating ramp of 1 K s^{-1}. H_2 from the background was found not to adsorb or react with the surface under our experimental conditions.

2.2. Density functional theory (DFT)

To examine the atomistic behavior of the system in question, DFT calculations were performed in which the interaction of water with the "29" oxide was modeled. The "29" oxide model structure used in these calculations was taken from previous studies [24,25] and consists of 4 atomic layers of metallic Cu(1 1 1) on which a single Cu_2O layer was placed. This oxide thin film is made up of fused hexagonal rings, each with six Cu atoms and six O atoms, buckling with linear O-Cu-O bonds. Additionally, we found that five O adatoms placed in the center on the hexagonal rings on the exposed Cu (1 1 1) surface were necessary in order to reproduce the experimental STM images of the "29" oxide [24]. Note that during optimizations, the bottom two Cu layers were held fixed in their bulk positions and all other atoms where allowed to relax.

All DFT calculations were performed using the Vienna *ab initio* Simulation Package (VASP) [50,51], which employs the projector augmented wave (PAW) method to project the pseudo core-electron wavefunctions onto the atomic centers [52–54]. Standard PAW projection sets released prior to 2012 were used in these calculations for all atoms. A cutoff energy of 500 eV was used for the determination of the plane-wave basis set. Throughout all calculations, wavefunctions were converged until total energy changes were $<10^{-6}$ eV and geometries were considered optimized when all interatomic forces were <0.02 eV/Å. A $(1 \times 2 \times 1)$ Monkhorst-Pack grid was used to sample the Brillouin zone in all calculations. The exchange-correlation energy was treated under the generalized gradient approximation (GGA) using the optB88-vdW functional [55,56] to compute water adsorption energies on the "29" oxide to capture nonlocal interactions. The "29" oxide was modeled as described previously [24], by a $\sqrt{13}R46.1$ Å $\times$ $7R21.8$ Å supercell, with (1×1) repetition, consisting of an oxide layer on the Cu(1 1 1) surface with that was four layers thick, where the bottom two layers of the slab were kept fixed in their bulk positions. This supercell is nearly rectangular with approximate dimensions of 18 Å by 9 Å.

Adsorption energies presented here were calculated using DFT energies. The contribution from zero-point energetics has been assessed in the Supplementary Content and is deemed negligible. Reaction barriers were also computed in VASP using the climbing image nudged elastic band (CINEB) [57,58] method to determine the transition state structure along with the associated reaction pathway energetics. Force optimizations along the pathway were handled using the fast inertial relaxation engine (FIRE) algorithm [59,60]. The Perdew-Burke-Ernzerhof (PBE) functional [61] was employed during reaction barrier calculations for all initial, transition, and final states, which optimized computational efficiency. All transition state structures were verified to have a single imaginary mode through vibrational analysis, with the wavefunction convergence criteria set to 10^{-8} eV and finite difference step sizes of 0.01 Å for the Hessian matrix construction. During the vibrational calculations, all copper layers were held fixed and vibrational modes corresponding to the "29" oxide layer, Pt atom, and adsorbed species were computed. The vibrational analysis was performed in part using homemade programs to process force outputs so as to create and diagonalize the dynamical matrix (following symmetrization), which allowed for parallelization of the necessary quantum chemical calculations.

3. Results and discussion

The desorption of water from the "29" oxide surface over a range of initial water coverages is shown in Fig. 1A, where 1 ML is defined as the saturation of the monolayer desorption peak. On weak binding metallic surfaces, such as Cu(1 1 1), water growth

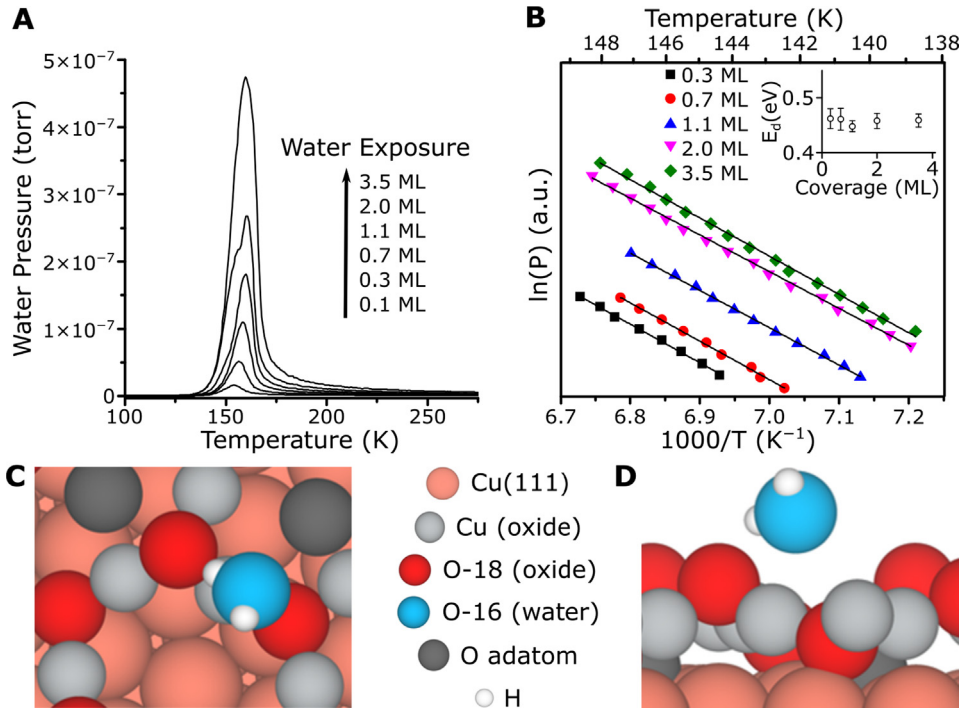

Fig. 1. (A) Family of TPD curves for various exposures of water on the "29" oxide. (B) Leading edge analysis of the water desorption curves. (C) Top view and (D) side view of DFT optimized structure of a water molecule bound to the "29" oxide.

is often 3-dimensional due to the strength of the water intermolecular hydrogen-bonds. Therefore, a complete single layer of water does not form, leading to a single zero-order water desorption feature in TPD experiments [62]. However, on the surfaces of bulk oxides water does have a tendency to form monolayer structures, due to stronger binding via hydrogen-bonds with surface layer O or hydroxyl species [37–43]. In this case, the thin "29" oxide Cu_2O-like film appears to bind water just strongly enough to form a monolayer, as two desorption features are seen in Fig. 1A. Leading edge analysis, or Habenschaden-Küppers analysis [63], was applied to the TPD curves to extract energetic information, and is shown in Fig. 1B. The inset in Fig. 1B shows the calculated desorption barrier for water from the TPD data, with the error in the best-fit line shown. It can be seen that the binding strength of water in the multilayer and monolayer coverage regimes are very similar. In the monolayer coverage regime, the desorption barrier of water was calculated to be 0.46 ± 0.02 eV, which is close to the desorption barrier of water on metallic surfaces [62,64,65]. These results suggest that the "29" oxide binds water slightly more weakly than what was measured on Cu(1 1 1) and bulk Cu_2O, however water desorption on all three surfaces occurs within a similar temperature range (~150–180 K) [49,62].

In order to further investigate and quantify the binding of water to the "29" oxide, DFT calculation were performed. Water adsorption was tested at 18 different sites across the "29" oxide surface (see the Supplementary Content for the structures and the associated energetics). Shown in Fig. 1C and D are the top and side views, respectively, of a sample water adsorption structure on the "29" oxide surface as obtained from the DFT calculations. It is clear from Fig. 1C that the water molecule prefers to be oriented above the Cu cation in the "29" oxide surface. However, Fig. 1D shows that the water molecule is slightly lifted from the surface and is hydrogen-bonding with the nearby O atom in the oxide layer. This binding motif was found to be the most favorable geometry for water adsorption across the tested adsorption sites. In this configuration, a lone-pair of electrons of the O in the water molecule bind to a surface Cu cation while also hydrogen-bonding with a surface O anion. The average calculated adsorption energy of water to the surface over all tested sites is −0.42 ± 0.10 eV, which is in good agreement with the experimentally determined desorption barrier of water (0.46 ± 0.02 eV). During these calculations, the adsorbed water induced energetically favorable defects in the oxide structure. This defect was accounted for appropriately in the adsorption energy calculations and the defective oxide was used as the basis for all subsequent calculations. Further discussion regarding this defect can be found in the Supplementary Content. Finally, we also find that our PBE-computed adsorption energy value of −0.47 eV for water at its most favorable binding site on the bare "29" oxide (see Supplementary Content) is stronger than on Cu(1 1 1) and on bulk Cu_2O, which have GGA reported computed values of −0.24 eV and −0.39 eV, respectively [66,67].

The TPD data in Fig. 1 shows that all water desorbs at low temperature from the "29" oxide surface. With the water desorption behavior from the "29" oxide characterized, it serves as an ideal surface for understanding water interactions with supported Pt species. Water desorption from extended Pt surfaces is generally higher in temperature [68–76], which allows for the deconvolution of water desorption from the "29" oxide and supported Pt. The nature of Pt growth on the "29" oxide has previously been characterized using CO as a probe molecule in surface science experiments, including TPD, STM, and IR spectroscopy techniques [21]. In summary, this work found that Pt growth below 3% ML (in reference to the Pt coverage, 1 ML is defined as the packing density of Cu (1 1 1)) results in the exclusive formation of isolated Pt single atoms, above 3% ML of Pt small clusters form, and above 12% ML the Pt grows into 3-dimensional particles which resembling highly stepped extended Pt surfaces [21].

Water desorption from the bare "29" oxide and Pt-modified surfaces is shown in Fig. 2A for water coverages of ~0.1 ML. It is initially clear that as the Pt coverage is increased the desorption temperature of water also increases. The peak assignments in Fig. 2 follow previous studies of water desorption from extended

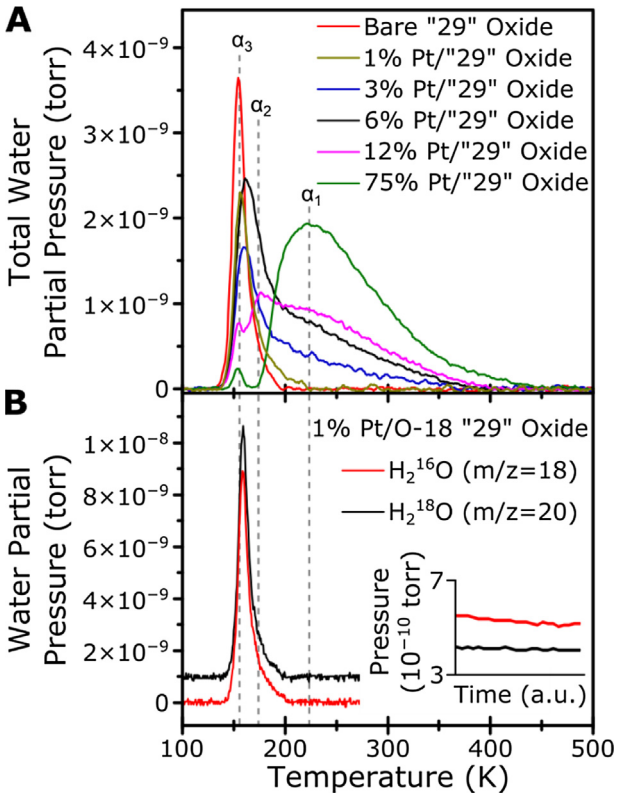

Fig. 2. (A) The desorption of ~0.1 ML of water from the "29" oxide with various coverages of Pt. (B) TPD experiment of 0.05 ML of water deposited on 1% Pt supported on O-18 labeled "29" oxide. Curves are offset for clarity. The inset shows the pressure of water isotopes during deposition.

Pt surfaces [68,69]. It is well accepted that Pt step sites bind water more strongly than terrace sites [70–76], and the binding strength of all Pt sites increases in the presence of surface bound O [77,78]. In accordance with previous studies, the α_1 peak is ascribed to recombinative desorption of OH on Pt steps (yielding gas phase water and surface bound O), α_2 is due to recombinative desorption of OH on Pt(1 1 1)-like terraces, and finally α_3 is due to the molecular desorption of water [68,69].

Shown in Fig. 2A, at 1% ML of Pt, at which coverage Pt exists as isolated single atoms, water desorbs molecularly from the surface (α_3). Water is bound with a similar strength to 1% ML of Pt as on the bare "29" oxide. To rationalize the desorption temperature of water from 1% ML Pt on the "29" oxide, DFT calculations of the adsorption of water to a Pt single atom were performed. The binding site for Pt on the "29" oxide has previously been proposed to reside in the Cu oxide ring that lacks an O adatom, which is detailed on our aforementioned previous work using STM and DFT with CO as a probe molecule [21]. At this single Pt atom site, water adsorption is calculated to be bound molecularly to the Pt atom with an adsorption energy of −0.44 eV. At this site, water binds primarily through a lone pair of electrons of the O atom to the Pt atom, with a hydrogen-bond to a neighboring O atom in the "29" oxide (discussed later in Fig. 5). As water adsorption is non-activated and bound molecularly, the similar calculated binding energy of water on Pt single atoms and the bare "29" oxide verifies the TPD results indicating that Pt single atoms and the bare "29" oxide have similar water binding strengths.

TPD experiments with Pt clusters were also performed, shown in Fig. 2A. Water desorption from the "29" oxide at Pt coverages of 3% and 6% ML is primarily molecular desorption, however, a desorption shoulder that is in line with the α_1 assignment (recombinative desorption of OH on Pt steps) also grows in as the Pt coverage increases [68,69]. This is evidence of the emergence of small Pt clusters that present surface sites similar to Pt step sites. As the Pt coverage is increased to 12% ML of Pt, the α_2 peak emerges, indicating that the Pt clusters have grown large enough to exhibit Pt terrace-like sites [68,69]. Finally at 75% ML of Pt, there is some molecular desorption of water, but the majority of water desorbs from the α_1 state. The water desorption peak from the 75% ML of Pt surface is also very broad, which can be explained by the heterogeneity of desorption sites and is consistent with the formation of highly stepped 3-dimensional Pt particles.

In order to probe the reactivity of the surface toward water activation, isotopic scrambling experiments were performed by forming the "29" oxide with O-18. The scrambling yield of $H_2^{16}O$ (m/z = 18) to $H_2^{18}O$ (m/z = 20) can be used as an indicator of water activation. Shown in Fig. 2B is the desorption of 0.05 ML of water from 1% ML of Pt on an O-18 labeled "29" oxide, at which coverage Pt exists as disperse single atoms. In order to accurately determine the amount for isotopic scrambling between the water and the oxide, the desorption of both $H_2^{16}O$ (m/z = 18) and $H_2^{18}O$ (m/z = 20) were monitored, shown in Fig. 2B and offset for clarity. The nature of the sample preparation requires large amounts of $^{18}O_2$ exposure in order to create the labeled "29" oxide support, and it was discovered that the high exposure of $^{18}O_2$ in the UHV chamber resulted in a larger background pressure of m/z = 20. The natural abundance of m/z = 20 water is <1%, which in this case can refer to either D_2O or $H_2^{18}O$. Therefore, within experimental error, any appreciable detection of m/z = 20 can be attributed to $H_2^{18}O$. In order to account for $H_2^{18}O$ adsorption from the background, the pressure of the water isotopes were monitored and the background was used as the water deposition source for the TPD experiments. The inset in Fig. 2B shows the pressure of $H_2^{16}O$ and $H_2^{18}O$ during water deposition by background exposure. It is clear that isotopic scrambling occurred as the surface exposure of $H_2^{16}O$ was greater, but there was more desorption of $H_2^{18}O$. In other words, the $H_2^{18}O$ (m/z = 20) to $H_2^{16}O$ (m/z = 18) ratio increases from exposure to desorption. It is also noteworthy that the low temperature desorption of water indicates that the water scrambling process occurs below 200 K.

A schematic model of water scrambling on the O-18 labeled "29" oxide surface is shown in Fig. 3. Moving from left to right, E_{18} and E_{20} are the number of water molecules of mass 18 ($H_2^{16}O$) and 20 ($H_2^{18}O$), respectively, exposed to the surface. After the exposed water is adsorbed to the $Cu_2^{18}O$ surface, the TPD experiment is performed to allow for water desorption. N_{18} and N_{20} are the number of molecules desorbed from the surface of mass 18 ($H_2^{16}O$) and 20 ($H_2^{18}O$), respectively. The $H_2^{16}O$ may be scrambled to $H_2^{18}O$ with some probability (P), while the rest ($1 - P$) would reversibly desorb as $H_2^{16}O$. All $H_2^{18}O$ will desorb as $H_2^{18}O$ (100%, shown as a probability of 1 in Fig. 3), regardless of if the water scrambled with O in the "29" oxide surface. From this simple logic, we derive the following equation:

$$P = \frac{N_{20}/N_{18} - E_{20}/E_{18}}{N_{20}/N_{18} + 1} \quad (1)$$

Therefore, by knowing the isotopic ratio of the reactants (E_{20}/E_{18}) and the products (N_{20}/N_{18}), the probability of water scrambling can be quantified. There should be no significant difference in sticking probability between isotopes of water, and

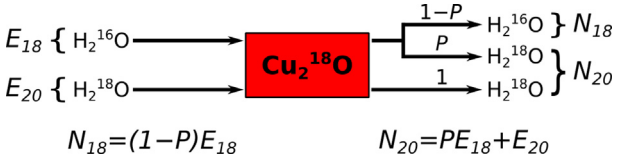

Fig. 3. Model for water scrambling on the isotopically labeled "29" oxide surface. The exposed $H_2^{18}O$ (E_{20}) is created in the chamber background.

therefore, the initial coverage of $H_2^{18}O$ to $H_2^{16}O$ on the surface (E_{20}/E_{18}) is proportional to the measured pressure ratio of $m/z = 20$ to $m/z = 18$ of the deposition source (i.e. the chamber background). The isotopic ratio of the desorbing water (N_{20}/N_{18}) is proportional to the ratio of $m/z = 20$ to $m/z = 18$ areas of the TPD peaks. Further discussion of the derivation of Eq. (1) can be found in the Supplementary Content.

The probability of water scrambling, calculated by Eq. (1), was studied as a function of total water coverage for different surfaces, shown in Fig. 4A. The Cu(1 1 1) surface served as a control for this experiment, as there is no O-18 on the surface to scramble with. As expected, no water scrambling was detected on Cu(1 1 1), and the ratio of $H_2^{16}O$ and $H_2^{18}O$ remained constant between the exposure and desorption. In the case of the bare "29" $Cu_2^{18}O$ film, water scrambling was detected at low coverage. As the water coverage is increased, the probability of scrambling decreases, which is consistent with a limited number of active sites that become titrated and leads to a higher probability of water desorption without isotopic scrambling. Possible active sites for water scrambling on the bare "29" oxide are the defect sites, which we have previously characterized and assigned as O vacancy and Cu adatom structures, which are the major two naturally occurring defects on the surface [79]. These results are in agreement with previous reports of defects in Cu_2O to be active for water dissociation [44].

The reactivity of Pt single atoms with water is of primary interest in this study, as water desorption from larger Pt clusters and extended surfaces has been previously studied and benchmarked [68–76]. Shown in Fig. 4A, the addition of single Pt atoms on the "29" oxide, the 1% Pt/$Cu_2^{18}O$/Cu(1 1 1) curve, shows an increase in water scrambling activity with respect to the bare "29" oxide surface. This is most noticeable at low water coverage values (<0.2 ML), where the water scrambling probability is greatest. For the 1% Pt/$Cu_2^{18}O$/Cu(1 1 1) surface at a water coverage of 0.027 ML the scrambling probability is 0.29, whereas for the bare $Cu_2^{18}O$/Cu (1 1 1) surface at a water coverage of 0.010 ML the scrambling probability is 0.14. The increased scrambling probability on the 1% Pt surface, despite a greater water coverage, demonstrates an increase in the number of active sites on the 1% Pt surface relative to the bare oxide. This is direct evidence that supported single Pt atoms are capable of water activation. As before, upon increasing the initial water coverage at a given Pt loading the water scrambling probability decreases, indicating a saturation of active sites that can only perform a limited number of water scrambling events in a single TPD experiment. As more Pt is added to the surface, Pt starts growing as 3-dimensional nanoparticles, adding more active sites on the surface for water scrambling and increasing the water scrambling activity. A similar comparison is made in Fig. 4B, which shows the scrambling probability of ~0.1 ML of water on the various examined surfaces. Some scrambling activity is found on the bare "29" oxide, and an increase is seen upon the addition of Pt which continues to increase as more Pt is added to the surface.

These experimental results are rationalized by our DFT calculations examining water activation on the bare "29" oxide and supported single Pt atoms. Shown in Fig. 5 is the proposed water scrambling pathway for a single Pt atom supported on the "29" oxide. Scrambling is initiated by cleavage of an O-H bond of the adsorbed water molecule. This process leads to a H adatom bound to an O of the "29" oxide and a hydroxyl on the single Pt atom. Using the PBE functional, this first step for O–H cleavage has a reaction energy (ΔE) of 0.42 eV and activation energy (E_a) of 0.43 eV.

It is initially obvious that Pt facilitates water activation by the dramatic reduction of the first O-H cleavage reaction energy and barrier with respect to the bare "29" oxide. Although, DFT calculations using the PBE functional (red line in Fig. 5) indicate that the forward reaction of water activation is not favored over water desorption. However, use of the optB88-vdW functional (blue lines in Fig. 5) give much more promising results for water dissociation. In the single Pt atom pathway, the optB88-vdW functional gives an adsorption energy of −0.44 eV for water on the single Pt atom, and a reaction energy of +0.41 eV for the initial water dissociation to a H adatom and hydroxyl on Pt. The difference in reaction energies for water dissociation using the vdW and PBE functionals are very small (~0.01 eV), within DFT error. For this reason, with a similar ΔE, E_a can be assumed similar between the two functionals [80]. It is reasonable to assume that the vdW functional would yield an activation energy for this elementary step similar to the calculated result using the PBE functional. This would indicate that the initiation of the scrambling pathway is competitive with, and slightly favored over, the reversible desorption of water from the "29" oxide.

The next step after the initial O–H cleavage in the proposed water scrambling pathway is a rearrangement of the hydroxyl on the Pt atom and surrounding oxide structure. This process consists of 4 separate elementary steps (see Supplementary Content), with an overall ΔE of 0.07 eV and moderate E_a of 0.15 eV, calculated with the PBE functional. The final state of the rearrangement of the hydroxyls is calculated to be near thermo-neutral (ΔE of 0.05 eV) with the desorption of water using the vdW functional. The most energetically costly process is the next reaction step, in which the H from the hydroxyl on the Pt atom is transferred to the O of the oxide. The PBE functional predicts an activation barrier of 0.52 eV, with a ΔE of 0.07 eV using the PBE functional and 0.03 eV with the vdW functional. This step is predicted to be rate limiting for the water scrambling, but indicates this atomistic picture of the water scrambling on the "29" oxide doped with single Pt atoms

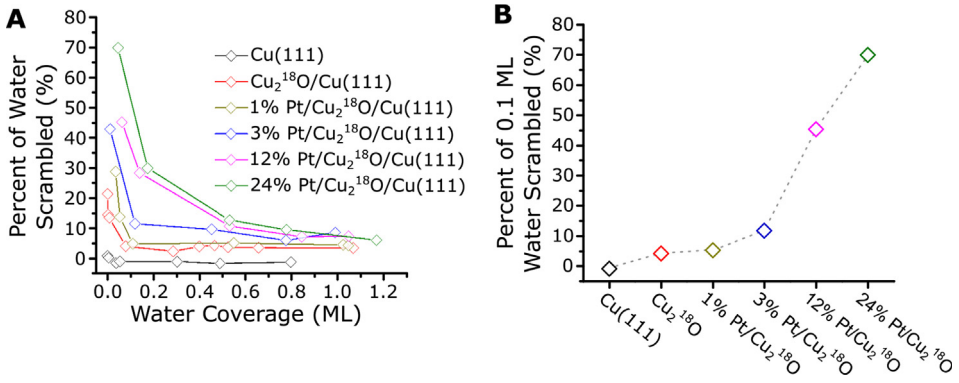

Fig. 4. (A) The probability of water scrambled for various surfaces as a function of water coverage. (B) The probability of water scrambled by the same surfaces at an initial water coverage of 0.1 ML.

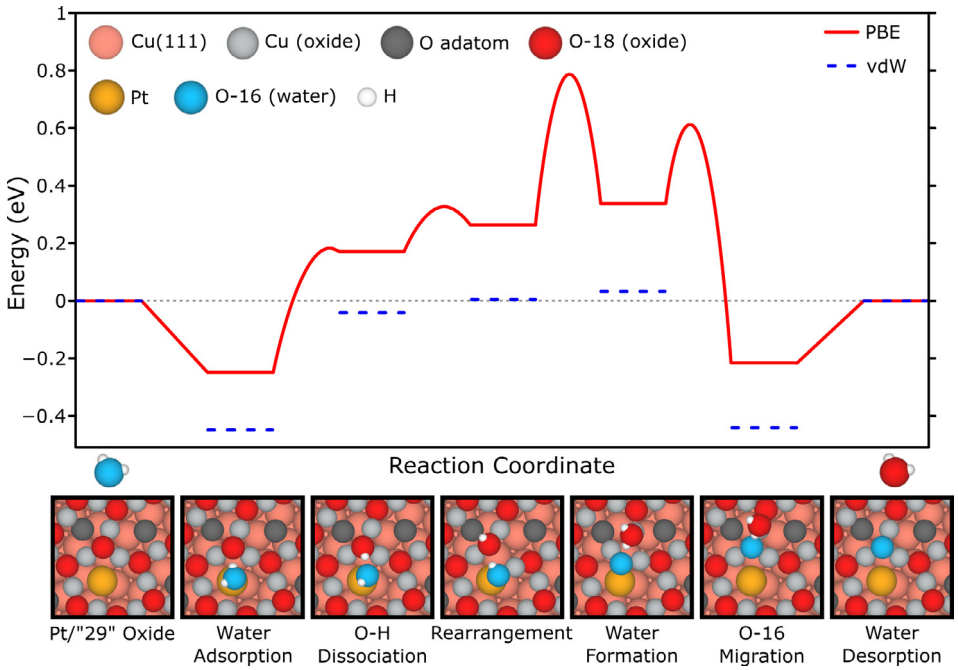

Fig. 5. DFT proposed reaction pathway for water scrambling by a Pt atom supported on the "29" oxide. Along the reaction coordinate are the calculated intermediates for each reaction step, which are also described below each image. The computed minimum energy pathways are given in the Supplementary Content.

is indeed plausible, as the E_a for the desorption of water in the initial adsorption configuration for this pathway is 0.44 eV using the vdW functional. The final reaction step to complete water scrambling involves the replacement of the O from the oxide with the O from water, resulting in adsorbed $H_2^{18}O$, and is exothermic. The PBE functional gives a ΔE of −0.55 eV, with an E_a of 0.27 eV, and the vdW functional finds a ΔE of −0.48 eV. As for the desorption of $H_2^{18}O$ from the surface, our calculations give a similar desorption barrier as the initial adsorption configuration of water, which is verified experimentally with overlapping $H_2^{18}O$ and $H_2^{16}O$ desorption peaks from both the bare "29" oxide and Pt single atoms in TPD experiments. Further calculations and discussion of reaction steps can be found in the Supplementary Content.

To further study the impact of the Pt single atom to the "29" oxide, the initial step of O-H cleavage was examined by further DFT calculations, shown in Fig. 6. As discussed above and shown in Fig. 5, the first step in this scrambling process is cleavage of a water O-H bond, resulting in a hydroxyl species on the single Pt atom and a hydrogen on an oxygen of the "29" oxide. In order to investigate the scrambling of water on the bare "29" oxide, a reaction barrier calculation for this elementary step without the Pt atom was carried out. The O–H bond cleavage was investigated by having the adsorbed water molecule (shown in Fig. 1) interact with the same oxygen anion in the "29" oxide as was investigated in Fig. 5. As shown in Fig. 6A, without the single Pt atom the reaction has an energy cost nearly twice as great, ΔE of 0.71 eV, with an E_a of 0.76 eV. Note that this reaction energy is consistent with O–H cleavage reaction energies over bulk Cu_2O [66]. In comparison to the activation energy over a single Pt atom of 0.43 eV, shown in Fig. 6B, it is clear that O-H cleavage over the intact bare "29" oxide is significantly less kinetically favorable. Additionally, when considering that the desorption barrier of water from the bare oxide is 0.45 eV whereas water activation is 0.76 eV, it can be concluded that water would completely desorb from the oxide before an O–H

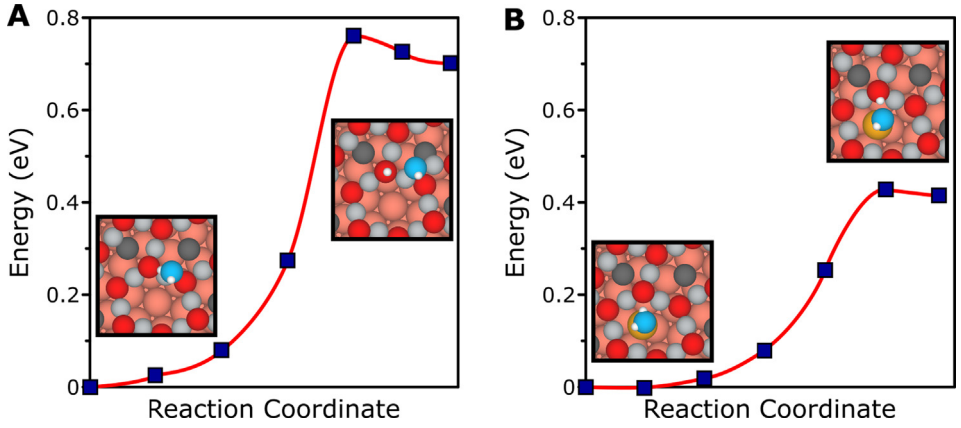

Fig. 6. Comparison of O–H bond cleavage (A) over the bare "29" oxide and (B) over a single Pt atom. We note that the computed desorption barrier over the bare oxide at this binding site 0.45 eV (see Supplementary Content), which is considerably lower than the O–H bond cleavage barrier of water over the bare oxide of 0.77 eV (see panel A). The labeling of the species is given in Fig. 5.

cleavage reaction. This justifies the low scrambling probability observed on the bare oxide, along with its occurrence only being possible at defect sites.

4. Conclusions

Water activation is a fundamental reaction step, playing an important role in many industrially relevant processes such as the water gas shift, steam reforming, and alcohol oxidation reactions. Using a model study approach, we found that single Pt atoms supported on the "29" copper oxide film exhibit the ability to activate water as evidenced experimentally via oxygen isotopic scrambling with the support. Coupled with the ability of Pt single atoms to oxidize CO, as recently reported [21], these surface science results support and shed light on previous real catalyst findings that highly dispersed Pt atoms on oxide supports are good water gas shift catalysts. We found that small amounts of isotopic scrambling occur on the bare copper oxide support due to defects, and the degree of scrambling is enhanced in the presence of Pt atoms. This is supported by theory for which a much lower activation energy barrier for O-H bond cleavage is obtained in the vicinity of Pt atoms as compared to the bare surface oxide support. A viable reaction pathway for water activation and scrambling at single Pt atom sites is proposed. DFT calculations also provide insight into the dynamic relationship between the adsorbate, single Pt atom, and oxide support in order for isotopic scrambling to occur. The results suggest that the Pt-oxide interface provides a high probability of water dissociation, which facilitates water scrambling, and this interface is maximized at the single Pt atom limit. As such, this study opens the door to follow up studies on the water gas shift reaction itself and, in particular, how water may assist in the low temperature oxidation of CO [21].

Acknowledgements

The surface science work at Tufts was supported by the Department of Energy BES under grant No. DE-FG02-05ER15730. M.M. thanks Tufts Chemistry for an Illumina Fellowship. Financial support to WSU was provided by the National Science Foundation CAREER program under contract No. CBET-1653561. A portion of the computer time for the computational work was performed using EMSL, a national scientific user facility sponsored by the Department of Energy's Office of Biological and Environmental Research and located at PNNL. PNNL is a multi-program national laboratory operated for the U.S. DOE by Battelle.

Appendix A. Supplementary material

Supplementary data associated with this article can be found, in the online version, at https://doi.org/10.1016/j.jcat.2018.04.024.

References

[1] S. Mitchell, J.M. Thomas, J. Pérez-Ramírez, Single atom catalysis, Catal. Sci. Technol. 7 (2017) 4248–4249, https://doi.org/10.1039/C7CY90090B.
[2] J. Liu, Catalysis by supported metal single atoms, ACS Catal. 7 (2017) 34–59, https://doi.org/10.1021/acscatal.6b01534.
[3] M. Flytzani-Stephanopoulos, B.C. Gates, Atomically dispersed supported metal catalysts, Annu. Rev. Chem. Biomol. Eng. 3 (2012) 545–574, https://doi.org/10.1146/annurev-chembioeng-062011-080939.
[4] M. Yang, M. Flytzani-Stephanopoulos, Design of single-atom metal catalysts on various supports for the low-temperature water-gas shift reaction, Catal. Today 298 (2017) 216–225, https://doi.org/10.1016/j.cattod.2017.04.034.
[5] C. Wang, M. Yang, M. Flytzani-Stephanopoulos, Single gold atoms stabilized on nanoscale metal oxide supports are catalytic active centers for various reactions, AlChE J. 62 (2015) 429–439, https://doi.org/10.1002/aic.
[6] M. Yang, J. Liu, S. Lee, B. Zugic, J. Huang, L.F. Allard, M. Flytzani-Stephanopoulos, A common single-site Pt(II)–O(OH)$_x$– species stabilized by sodium on "Active" and "Inert" supports catalyzes the water-gas shift reaction, J. Am. Chem. Soc. 137 (2015) 3470–3473, https://doi.org/10.1021/ja513292k.
[7] M. Flytzani-Stephanopoulos, Gold atoms stabilized on various supports catalyze the water-gas shift reaction, Acc. Chem. Res. 47 (2014) 783–792, https://doi.org/10.1021/ar4001845.
[8] M. Yang, S. Li, Y. Wang, J.A. Herron, Y. Xu, L.F. Allard, S. Lee, J. Huang, M. Mavrikakis, M. Flytzani-Stephanopoulos, Catalytically active Au-O(OH)$_x$-species stabilized by alkali ions on zeolites and mesoporous oxides, Science. 346 (2014) 1498–1501.
[9] Y. Zhai, D. Pierre, R. Si, W. Deng, P. Ferrin, A.U. Nilekar, G. Peng, J.A. Herron, D.C. Bell, H. Saltsburg, M. Mavrikakis, M. Flytzani-Stephanopoulos, Alkali-stabilized Pt-OH$_x$ species catalyze low-temperature water-gas shift reactions, Science 329 (2010) 1633–1636, https://doi.org/10.1126/science.1192449.
[10] Q. Fu, H. Saltsburg, M. Flytzani-Stephanopoulos, Active nonmetallic Au and Pt species on ceria-based water-gas shift catalysts, Science 301 (2003) 935–938, https://doi.org/10.1126/science.1085721.
[11] S. Aranifard, S.C. Ammal, A. Heyden, On the importance of metal-oxide interface sites for the water-gas shift reaction over Pt/CeO$_2$ catalysts, J. Catal. 309 (2014) 314–324, https://doi.org/10.1016/j.jcat.2013.10.012.
[12] S.C. Ammal, A. Heyden, Water–gas shift catalysis at corner atoms of Pt clusters in contact with a TiO$_2$(110) support surface, ACS Catal. 4 (2014) 3654–3662.
[13] S.C. Ammal, A. Heyden, Water-gas shift activity of atomically dispersed cationic platinum versus metallic platinum clusters on titania supports, ACS Catal. 7 (2017) 301–309, https://doi.org/10.1021/acscatal.6b02764.
[14] C.M.Y. Yeung, K.M.K. Yu, Q.J. Fu, D. Thompsett, M.I. Petch, S.C. Tsang, Engineering Pt in ceria for a maximum metal-support interaction in catalysis, J. Am. Chem. Soc. 127 (2005) 18010–18011, https://doi.org/10.1021/ja056102c.
[15] K. Ding, A. Gulec, A.M. Johnson, N.M. Schweitzer, G.D. Stucky, L.D. Marks, P.C. Stair, Identification of active sites in CO oxidation and water-gas shift over supported Pt catalysts, Science 350 (2015) 189–192, https://doi.org/10.1126/science.aac6368.
[16] L.C. Grabow, A.A. Gokhale, S.T. Evans, J.A. Dumesic, M. Mavrikakis, Mechanism of the water gas shift reaction on Pt: first principles, experiments, and microkinetic modeling, J. Phys. Chem. C. 4608–4617 (2008).
[17] J. Knudsen, A.U. Nilekar, R.T. Vang, J. Schnadt, E.L. Kunkes, J.A. Dumesic, M. Mavrikakis, F. Besenbacher, A Cu/Pt near-surface alloy for water-gas shift catalysis, J. Am. Chem. Soc. 129 (2007) 6485–6490, https://doi.org/10.1021/ja0700855.
[18] J. Kugai, J.T. Miller, N. Guo, C. Song, Oxygen-enhanced water gas shift on ceria-supported Pd-Cu and Pt-Cu bimetallic catalysts, J. Catal. 277 (2011) 46–53, https://doi.org/10.1016/j.jcat.2010.10.014.
[19] S. Liu, J.M. Tan, A. Gulec, L.A. Crosby, T.L. Drake, N.M. Schweitzer, M. Delferro, L. D. Marks, T.J. Marks, P.C. Stair, Stabilizing single-atom and small-domain platinum via combining organometallic chemisorption and atomic layer deposition, Organometallics 36 (2017) 818–828, https://doi.org/10.1021/acs.organomet.6b00869.
[20] L. DeRita, S. Dai, K. Lopez-Zepeda, N. Pham, G.W. Graham, X. Pan, P. Christopher, Catalyst architecture for stable single atom dispersion enables site-specific spectroscopic and reactivity measurements of CO adsorbed to Pt atoms, oxidized Pt clusters, and metallic Pt clusters on TiO$_2$, J. Am. Chem. Soc. 139 (2017) 14150–14165, https://doi.org/10.1021/jacs.7b07093.
[21] A.J. Therrien, A.J.R. Hensley, M.D. Marcinkowski, R. Zhang, F.R. Lucci, B. Coughlin, A.C. Schilling, J.-S. McEwen, E.C.H. Sykes, An atomic-scale view of single-site Pt catalysis for low-temperature CO oxidation, Nat. Catal. 1 (2018) 192–198, https://doi.org/10.1038/s41929-018-0028-2.
[22] F. Jensen, F. Besenbacher, I. Stensgaard, Two new oxygen induced reconstructions on Cu(111), Surf. Sci. 270 (1992) 400–404. http://www.sciencedirect.com/science/article/pii/003960289291282G.
[23] T. Matsumoto, R.A. Bennett, P. Stone, T. Yamada, K. Domen, M. Bowker, Scanning tunneling microscopy studies of oxygen adsorption on Cu(111), Surf. Sci. 471 (2001) 225–245, https://doi.org/10.1016/S0039-6028(00)00918-3.
[24] A.J. Therrien, R. Zhang, F.R. Lucci, M.D. Marcinkowski, A. Hensley, J.-S. McEwen, E.C.H. Sykes, Structurally accurate model for the "29"-structure of Cu$_x$O/Cu (111): a DFT and STM study, J. Phys. Chem. C 120 (2016) 10879–10886, https://doi.org/10.1021/acs.jpcc.6b01284.
[25] A.J.R. Hensley, A.J. Therrien, R. Zhang, M.D. Marcinkowski, F.R. Lucci, E.C.H. Sykes, J.-S. McEwen, CO adsorption on the "29" Cu$_x$O/Cu(111) surface: an integrated DFT, STM and TPD study, J. Phys. Chem. C. 120 (2016) 25387–25394, https://doi.org/10.1021/acs.jpcc.6b07670.
[26] F. Besenbacher, J.K. Nørskov, Oxygen chemisorption on metal surfaces: general trends for Cu, Ni and Ag, Prog. Surf. Sci. 44 (1993) 5–66, https://doi.org/10.1016/0079-6816(93)90006-H.
[27] D.S. Newsome, The water-gas shift reaction, Catal. Rev. 21 (1980) 275–318, https://doi.org/10.1080/03602458008067535.
[28] C.V. Ovesen, P. Stoltze, J.K. Nørskov, C.T. Campbell, A kinetic model of the water gas shift reaction, J. Catal. 134 (1992) 445–468, https://doi.org/10.1016/0021-9517(92)90334-E.
[29] O. Jakdetchai, T. Nakajima, Mechanism of the water-gas shift reaction over Cu (110), Cu(111) and Cu(100) surfaces: an AM1-d study, J. Mol. Struct. Theochem. 619 (2002) 51–58, https://doi.org/10.1016/S0166-1280(02)00410-4.
[30] X. Deng, A. Verdaguer, T. Herranz, C. Weis, H. Bluhm, M. Salmeron, Surface chemistry of Cu in the presence of CO$_2$ and H$_2$O, Langmuir. 24 (2008) 9474–9478, https://doi.org/10.1021/la8011052.
[31] J.A. Rodriguez, J. Graciani, J. Evans, J.B. Park, F. Yang, D. Stacchiola, S.D. Senanayake, S. Ma, M. Perez, P. Liu, J.F. Sanz, J. Hrbek, Water-gas shift reaction

on a highly active inverse CeO_x/Cu(111) catalyst: unique role of ceria nanoparticles, Angew. Chemie - Int. Ed. 121 (2009) 8191–8194, https://doi.org/10.1002/anie.200903918.
[32] S.D. Senanayake, D. Stacchiola, J.A. Rodriguez, Unique properties of ceria nanoparticles supported on metals: novel inverse and the water-gas shift reaction, Acc. Chem. Res. 46 (2013) 1702–1711, https://doi.org/10.1021/ar300231p.
[33] W. An, F. Xu, D. Stacchiola, P. Liu, Potassium-induced effect on the structure and chemical activity of the Cu_xO/Cu(111) ($x \leq 2$) surface: a combined scanning tunneling microscopy and density functional theory study, ChemCatChem. 7 (2015) 3865–3872, https://doi.org/10.1002/cctc.201500719.
[34] A.A. Gokhale, J.A. Dumesic, M. Mavrikakis, On the mechanism of low-temperature water gas shift reaction on copper, J. Am. Chem. Soc. 130 (2008) 1402–1414, https://doi.org/10.1021/ja0768237.
[35] N. Takezawa, N. Iwasa, Steam reforming and dehydrogenation of methanol: difference in the catalytic functions of copper and group VIII metals, Catal. Today 36 (1997) 45–56, https://doi.org/10.1016/S0920-5861(96)00195-2.
[36] A.Y. Rozovskii, G.I. Lin, Fundamentals of methanol synthesis and decomposition, Top. Catal. 22 (2003) 137–150. http://link.springer.com/article/10.1023/A:1023555415577.
[37] M.A. Henderson, The interaction of water with solid surfaces: fundamental aspects revisited, Surf. Sci. Rep. 46 (2002) 1–308, https://doi.org/10.1016/S0167-5729(01)00020-6.
[38] G.E. Ewing, Ambient thin film water on insulator surfaces, Chem. Rev. 106 (2006) 1511–1526, https://doi.org/10.1021/cr040369x.
[39] O. Bjorneholm, M.H. Hansen, A. Hodgson, L.-M. Liu, D.T. Limmer, A. Michaelides, P. Pedevilla, J. Rossmeisl, H. Shen, G. Tocci, E. Tyrode, M.-M. Walz, J. Werner, H. Bluhm, Water at interfaces, Chem. Rev. 116 (2016) 7698–7726, https://doi.org/10.1021/acs.chemrev.6b00045.
[40] G.E. Brown, V.E. Henrich, W.H. Casey, D.L. Clark, C. Eggleston, A. Felmy, D.W. Goodman, M. Grtzel, G. Maciel, M.I. Mccarthy, K.H. Nealson, D.A. Sverjensky, M.F. Toney, J.M. Zachara, Metal oxide surfaces and their interactions with aqueous solutions and microbial organisms microbial organisms, Chem. Rev. 99 (1999) 77–174, https://doi.org/10.1021/cr980011z.
[41] M. Salmeron, H. Bluhm, M. Tatarkhanov, G. Ketteler, T.K. Shimizu, A. Mugarza, X. Deng, T. Herranz, S. Yamamoto, A. Nilsson, Water growth on metals and oxides: binding, dissociation, and role of hydroxyl groups, Faraday Discuss. 141 (2009) 221–229, https://doi.org/10.1039/B816684F.
[42] P. Dementyev, K.-H. Dostert, F. Ivars-Barceló, C.P. O'Brien, F. Mirabella, S. Schauermann, X. Li, J. Paier, J. Sauer, H.-J. Freund, Water interaction with iron oxides, Angew. Chemie Int. Ed. 54 (2015) 13942–13946, https://doi.org/10.1002/anie.201506439.
[43] R. Mu, Z.-j. Zhao, Z. Dohnálek, J. Gong, structural motifs of water on metal oxide surfaces, Chem. Soc. Rev. 46 (2017) 1785–1806, https://doi.org/10.1039/C6CS00864J.
[44] K. Mudiyanselage, S.D. Senanayake, P.J. Ramirez, S. Kundu, A.E. Baber, F. Yang, S. Agnoli, S. Axnanda, Z. Liu, J. Hrbek, J. Evans, J.A. Rodriguez, D. Stacchiola, Intermediates arising from the water–gas shift reaction over Cu surfaces: from UHV to near atmospheric pressures Top, Catal. 58 (2015) 271–280, https://doi.org/10.1021/ar300231p.
[45] J.H. Stenlid, M. Soldemo, A.J. Johansson, C. Leygraf, M. Göthelid, J. Weissenrieder, T. Brinck, Reactivity at the $Cu_2O(100)$:Cu–H_2O interface: a combined DFT and PES study, Phys. Chem. Chem. Phys. 18 (2016) 30570–30584, https://doi.org/10.1039/C6CP04410G.
[46] C.X. Kronawitter, C. Riplinger, X. He, P. Zahl, E.A. Carter, P. Sutter, B.E. Koel, Hydrogen-bonded cyclic water clusters nucleated on an oxide surface, J. Am. Chem. Soc. 136 (2014) 13283–13288.
[47] C. Riplinger, E.A. Carter, Cooperative effects in water binding to cuprous oxide surfaces, J. Phys. Chem. C 119 (2015) 9311–9323, https://doi.org/10.1021/acs.jpcc.5b00383.
[48] I.D. Petsalakis, G. Theodorakopoulos, J. Whitten, Electronic structure and spectra of $(Cu_2O)_n$-H_2O complexes, Phys. Chem. Chem. Phys. 17 (2015) 428–433, https://doi.org/10.1039/C4CP04303K.
[49] A. Önsten, J. Weissenrieder, D. Stoltz, S. Yu, M. Göthelid, U.O. Karlsson, Role of defects in surface chemistry on $Cu_2O(111)$, J. Phys. Chem. C. 117 (2013) 19357–19364.
[50] G. Kresse, J. Furthmüller, Efficient iterative schemes for ab initio total-energy calculations using a plane-wave basis set, Phys. Rev. B 54 (1996) 11169–11186, https://doi.org/10.1103/PhysRevB.54.11169.
[51] G. Kresse, J. Hafner, Ab initio molecular dynamics for liquid metals, Phys. Rev. B 47 (1993) 558–561, https://doi.org/10.1103/PhysRevB.47.558.
[52] P.E. Blöchl, Projector augmented-wave method, Phys. Rev. B 50 (1994) 17953–17979, https://doi.org/10.1103/PhysRevB.50.17953.
[53] G. Kresse, D. Joubert, From ultrasoft pseudopotentials to the projector augmented-wave method, Phys. Rev. B 59 (1999) 1758–1775, https://doi.org/10.1103/PhysRevB.59.1758.
[54] J.D. Pack, H.J. Monkhorst, Special points for Brillouin-zone integrations, Phys. Rev. B. 13 (1976) 5188–5192, https://doi.org/10.1103/PhysRevB.16.1748.
[55] J. Klimeš, D.R. Bowler, A. Michaelides, Chemical accuracy for the van der waals density functional, J. Phys. Condens. Matter. 22 (2010) 22201, https://doi.org/10.1088/0953-8984/22/2/022201.
[56] J. Klimeš, D.R. Bowler, A. Michaelides, Van der waals density functionals applied to solids, Phys. Rev. B. 83 (2011) 195131, https://doi.org/10.1103/PhysRevB.83.195131.
[57] G. Henkelman, H. Jónsson, Improved tangent estimate in the nudged elastic band method for finding minimum energy paths and saddle points, J. Chem. Phys. 113 (2000) 9978–9985, https://doi.org/10.1063/1.1323224.
[58] G. Henkelman, B.P. Uberuaga, H. Jónsson, Climbing image nudged elastic band method for finding saddle points and minimum energy paths, J. Chem. Phys. 113 (2000) 9901–9904, https://doi.org/10.1063/1.1329672.
[59] E. Bitzek, P. Koskinen, F. Gähler, M. Moseler, P. Gumbsch, Structural relaxation made simple, Phys. Rev. Lett. 97 (2006) 170201, https://doi.org/10.1103/PhysRevLett. 97.170201.
[60] D. Sheppard, R. Terrell, G. Henkelman, Optimization methods for finding minimum energy paths, J. Chem. Phys. 128 (2008) 134106, https://doi.org/10.1063/1.2841941.
[61] J.P. Perdew, K. Burke, M. Ernzerhof, Generalized gradient approximation made simple, Phys. Rev. Lett. 77 (1996) 3865–3868, https://doi.org/10.1103/PhysRevLett.77.3865.
[62] B.J. Hinch, L.H. Dubois, Stable and metastable phases of water adsorbed on Cu (111), J. Chem. Phys. 96 (1992) 3262–3268, https://doi.org/10.1063/1.461971.
[63] E. Habenschaden, J. Küppers, Evaluation of flash desorption spectra, Surf. Sci. 138 (1984) L147–L150, https://doi.org/10.1016/0167-2584(84)90346-3.
[64] R.H. Stulen, P.A. Thiel, Electron-stimulated desorption and thermal desorption spectrometry of H_2O on nickel (111), Surf. Sci. 157 (1985) 99–118, https://doi.org/10.1016/0039-6028(85)90638-7.
[65] C.T. Campbell, K.A. Daube, A surface science investigation of the water-gas shift reaction on Cu(111), J. Catal. 104 (1987) 109–119, https://doi.org/10.1016/0021-9517(87)90341-1.
[66] S.A. Saraireh, M. Altarawneh, Density functional theory periodic slab calculations of adsorption and dissociation of H_2O on the $Cu_2O(110)$:CuO surface, Can. J. Phys. 91 (2013) 1101–1106, https://doi.org/10.1139/cjp-2013-0272.
[67] A. Michaelides, V.A. Ranea, P.L. de Andres, D.A. King, General model for water monomer adsorption on close-packed transition and noble metal surfaces, Phys. Rev. Lett. 90 (2003) 216102, https://doi.org/10.1103/PhysRevLett.90.216102.
[68] M.J.T.C. van der Niet, A. den Dunnen, L.B.F. Juurlink, M.T.M. Koper, Co-adsorption of O and H_2O on nanostructured platinum surfaces: does OH form at steps?, Angew Chemie 122 (2010) 6722–6725, https://doi.org/10.1002/ange.201002124.
[69] M.J.T.C. van der Niet, A. den Dunnen, L.B.F. Juurlink, M.T.M. Koper, The influence of step geometry on the desorption characteristics of O_2, D_2, and H_2O from stepped Pt surfaces, J. Chem. Phys. 132 (2010) 174705, https://doi.org/10.1063/1.3407434.
[70] M.J. Kolb, R.G. Farber, J. Derouin, C. Badan, F. Calle-Vallejo, L.B.F. Juurlink, D.R. Killelea, M.T.M. Koper, Double-stranded water on stepped platinum surfaces, Phys. Rev. Lett. 116 (2016) 136101, https://doi.org/10.1103/PhysRevLett.116.136101.
[71] M. Morgenstern, T. Michely, G. Comsa, Anisotropy in the adsorption of H_2O at low coordination sites on Pt(111), Phys. Rev. Lett. 77 (1996) 703–706, https://doi.org/10.1103/PhysRevLett. 77.703.
[72] O. Endo, M. Nakamura, R. Sumii, K. Amemiya, 1D hydrogen bond chain on Pt (211) stepped surface observed by O K-NEXAFS spectroscopy, J. Phys. Chem. C 116 (2012) 13980–13984, https://doi.org/10.1021/jp302509k.
[73] R. Peköz, S. Wörner, L.M. Ghiringhelli, D. Donadio, Trends in the adsorption and dissociation of water clusters on flat and stepped metallic surfaces, J. Phys. Chem. C 118 (2014) 29990–29998, https://doi.org/10.1021/jp510242h.
[74] S. Meng, E. Wang, S. Gao, Water adsorption on metal surfaces: a general picture from density functional theory studies, Phys. Rev. B 69 (2004) 195404, https://doi.org/10.1103/PhysRevB.69.195404.
[75] M.J. Kolb, F. Calle-Vallejo, L.B.F. Juurlink, M.T.M. Koper, Density functional theory study of adsorption of H_2O, H, O, and OH on stepped platinum surfaces, J. Chem. Phys. 140 (2014) 134708, https://doi.org/10.1063/1.4869749.
[76] A. den Dunnen, M.J.T.C. van der Niet, C. Badan, M.T.M. Koper, L.B.F. Juurlink, Long-range influence of steps on water adsorption on clean and D-covered Pt surfaces, Phys. Chem. Chem. Phys. 17 (2015) 8530–8537, https://doi.org/10.1039/C4CP03165B.
[77] C. Clay, S. Haq, A. Hodgson, Hydrogen bonding in mixed OH + H_2O overlayers on Pt(111), Phys. Rev. Lett. 92 (2004) 46102, https://doi.org/10.1103/PhysRevLett.92.046102.
[78] J.R. Creighton, J.M. White, SIMS and TDS study of the reaction of water and oxygen on Pt(111), Surf. Sci. 122 (1982) L648–L652, https://doi.org/10.1116/1.572287.
[79] A.J. Therrien, A.J.R. Hensley, R. Zhang, A. Pronschinske, M.D. Marcinkowski, J.-S. McEwen, E.C.H. Sykes, Characterizing the geometric and electronic structure of defects in the "29" copper surface oxide, J. Chem. Phys. 147 (2017) 224706, https://doi.org/10.1063/1.4996729.
[80] A.J.R. Hensley, Y. Wang, J.-S. McEwen, Phenol deoxygenation mechanisms on Fe(110) and Pd(111), ACS Catal. 5 (2015) 523–536, https://doi.org/10.1021/cs501403w.